

Aqueous Humor Metabolomics in Different Stages of Diabetic Retinopathy Based on Ultra - Performance Liquid Chromatography - Tandem Mass Spectrometry

Zetong Nie^{1,*}, Shaofang Pang^{1,*}, Zhaoxiong Wang^{2,*}, Meng Yang¹, Xiang Zhang¹, Haoxin Guo¹, Wenbo Li¹, Boshi Liu¹, Weihong Yu³, Bojie Hu¹ 

¹Tianjin Key Laboratory of Retinal Functions and Diseases, Tianjin Branch of National Clinical Research Center for Ocular Disease, Eye Institute and School of Optometry, Tianjin Medical University Eye Hospital, Tianjin, People's Republic of China; ²Department of Ophthalmology, Tianjin Baodi Hospital, Tianjin, People's Republic of China; ³Department of Ophthalmology, Peking Union Medical College Hospital, Chinese Academy of Medical Sciences Key Laboratory of Ocular Fundus Diseases, Chinese Academy of Medical Sciences, Beijing, People's Republic of China

*These authors contributed equally to this work

Correspondence: Bojie Hu, Tianjin Medical University Eye Hospital, No. 251, Fukang Road, Nankai District, Tianjin, 300384, People's Republic of China, Email bhu07@tmu.edu.cn; Weihong Yu, Peking Union Medical College Hospital, No. 1 Shuaifuyuan Wangfujing Dongcheng District, Beijing, 100730, People's Republic of China, Email yuweihongpumch@163.com

Purpose: To search for differential metabolites in patients with proliferative diabetic retinopathy (PDR), patients with nonproliferative diabetic retinopathy (NPDR), and control subjects, and to study their potential biomarkers in depth.

Patients and Methods: An untargeted metabolomic approach based on ultra-performance liquid chromatography-tandem mass spectrometry was used to study aqueous humor from 63 patients with PDR, 37 patients with NPDR, and 30 non-diabetic controls. Differential metabolites in different periods of diabetic retinopathy (DR) were identified using orthogonal projections to latent structure discriminant analysis and fold-change. Further logistic regression and receiver operating characteristic curve analysis were performed to select and validate potential biomarkers.

Results: Compared to the control group, the PDR group had 80 differential metabolites, among which 3-methylhistamine, N-acetyl-L-histidine, and cytosine were identified as potential biomarkers, whereas the NPDR group had 94 differential metabolites, among which and N-acetyl-L-histidine and hypoxanthine were identified as potential biomarkers. Relative to the PDR and NPDR groups, 5-hydroxyindole-3-acetic acid and L-3-hydroxykynurenine may be potential biomarkers suggesting DR developmental stage or progression.

Conclusion: The metabolite profiles identified in this study provide insights into the mechanisms of DR onset and progression in future studies and may eventually inform the development of metabolic biomarkers for prognosis and new therapeutic strategies for DR management.

Keywords: diabetic retinopathy, metabolomics, biomarkers, ultra-performance liquid chromatography-tandem mass spectrometry

Introduction

The prevalence of diabetes mellitus (DM) is increasing worldwide and DM is the most prevalent disease in China. With a global surge in the incidence of DM in recent years, the number of people with diabetic retinopathy (DR) is expected to reach 191 million by 2030.¹ DR, a common ocular complication of DM, is a major cause of blindness and visual impairment in working age.² DR is classified into non-proliferative diabetic retinopathy (NPDR) and proliferative diabetic retinopathy (PDR) based on the presence of neovascularization.³ A longer duration of DM and poor glycemic control are the main risk factors for DR development and progression, but the pathogenesis remains obscured. Therefore,

understanding the pathophysiological mechanisms at different stages of DR development is important for DR prevention and treatment.⁴

Aqueous humor (AH) specimens are easier to obtain than vitreous specimens and provide favorable conditions for studying differential metabolites in DR patients at different times,⁵ which is conducive to improving the understanding of the molecular mechanisms of diabetic retinopathy. The metabolic characteristics of AH include (1) active pumping of metabolites into the AH against a concentration gradient; and (2) metabolites are produced by avascular tissues in communication with the AH and are consumed faster than they enter the AH.⁶

Nuclear magnetic resonance (NMR) spectrometry and mass spectrometry (MS) are the main research techniques in metabolomics. Although NMR is non-invasive and requires a smaller sample size, it is less sensitive and reliable; therefore, it has less clinical application.⁷ Currently, the most widely used techniques combine mass spectrometry and chromatography, including gas chromatography-mass spectrometry (GC-MS), liquid chromatography-mass spectrometry (LC-MS), and liquid chromatography-nuclear magnetic-mass spectrometry (LC-NMR-MS).^{8,9}

DR pathogenesis is associated with persistent metabolic disturbances, inflammation, and oxidative stress induced by hyperglycemia.¹⁰ A summary of existing studies showed that the classification of metabolites in DR focuses on amino acids, organic acids, sugars, and organic salts, and to a lesser extent, nucleic acids, polyols, and acylcarnitines.¹ Jin conducted an untargeted metabolomics study by NMR on AH samples from patients with DR, patients with DM, and elderly patients with cataracts and identified eight characteristic differential metabolites, including significantly elevated dimethylarginine levels, which revealed abnormalities in amino acid metabolic pathways in patients with DR and suggested the pathophysiological processes of mitochondrial dysfunction and oxidative stress.¹¹ Ascorbic acid levels were significantly lower in patient AH, vitreous fluid, and serum.^{4,12,13} Islam found that ascorbic acid inhibited tumor angiogenesis. Therefore, ascorbic acid may be associated with DR angiogenesis.¹⁴ Sumarriva compared the differential metabolic profiles of patients with PDR and NPDR, reporting significant differences in the oxidation of saturated fatty acids, fatty acids, and vitamin D3 metabolism, with carnitine the key factor contributing to the differences in numerous metabolic pathways.¹⁵

Metabolomics provides valuable insights into the biomarkers of DR. Currently, metabolomic analyses of different stages of DR primarily focus on serum metabolomics. Metabolomics of AH can offer a more comprehensive and direct perspective. The present study applied an untargeted metabolomics approach using ultra-performance liquid chromatography-tandem mass spectrometry (UPLC-MS/MS) combined with multivariate statistical analysis to explore the characteristic metabolic profile of AH in patients with different stages of DR, focusing on the metabolic heterogeneity in the AH in patients with PDR and NPDR, and to investigate in depth the potential biomarkers in AH during DR onset and progression.

Methods

Patients and Subgroups

This study was approved by the Human Investigation Ethics Committee of the Eye Hospital of Tianjin Medical University and was conducted in accordance with the principles of the Declaration of Helsinki. All patients provided informed consent before study inclusion.

We recruited 130 patients from the Eye Centre of Peking Union Medical College Hospital, the Eye Hospital of Tianjin Medical University, and the Fourth Hospital of Hebei Medical University from 2019 to 2022. All participants were screened according to the uniform diagnostic criteria or consensus of the Chinese Society of Fundus Diseases.

The inclusion criteria for the disease group (n=100) were a confirmed diagnosis of type 2 DM and the presence of DR, as determined by fundus dilatation examination by an experienced retinal specialist. The disease group was divided into PDR (n=63) and NPDR (n=37) groups based on the Early Treatment Diabetic Retinopathy Study criteria. PDR was diagnosed based on the presence of retinal neovascularization and additional clinical signs such as vitreous hemorrhage or retinal detachment. NPDR was diagnosed based on the presence of spotty bleeding, microaneurysms, cotton wool spots, or microvascular abnormalities within the retina. Patients with age-related cataracts without diabetes mellitus

(based on LOCS II grading criteria) were selected as the control group (n=30), and cataracts caused by other factors such as concurrent, traumatic, pharmacologic, and metabolic were excluded.

Subgroups were formed according to the presence or absence of a history of retinal laser treatment. Patients with PDR (n=63) were divided into laser (n=21) and non-laser (n=32) groups, excluding those for whom whether retinal laser photocoagulation had been performed was unknown (n=10). PDR patients (n=63) were divided into group a (DM <10 years) (n=20), group b (10 ≤ DM <20 years) (n=23), and group c (DM ≥20 years) (n=20) according to the DM duration.

All subjects meeting the following criteria were excluded: (1) patients with type 1 DM; (2) patients with a history of previous ocular surgery; (3) patients with previous vitreous injection <1 month previously; (4) patients with other ocular diseases (uveitis, central or branch retinal vein obstruction, age-related macular degeneration, glaucoma, etc.); and (5) patients with severe heart, liver, or kidney diseases.

Sample Collection and Preparation

The AH samples were collected under the same aseptic operating conditions. At the beginning of the surgical intervention, approximately 0.15 mL of AH was collected using a 1 mL syringe by surgical microscopy. A 50-μL sample of AH was immediately mixed with 150 μL of cold methanol/ethanol (v/v, 1:1) and vortexed for 30 seconds. The mixture was incubated at -20°C overnight and centrifuged at 4°C for 10 min at 14000g. The supernatants were immediately transferred into 0.2 mL high-performance liquid chromatography (HPLC) vials and stored at -80 °C until analysis.

UPLC-MS/MS Analysis

The AH metabolite separation and analysis were performed using a Waters ACQUITY UPLC system coupled to a Q Exactive Orbitrap mass spectrometer (Thermo Scientific, Waltham, MA, USA). An Acquity UPLC (Waters, USA) liquid system coupled to a BEH Amide analytical column (1.0 mm × 100 mm, 1.7 μm particle size; Waters, Milford, MA) at 35 °C was used for liquid chromatography separation. The flow rate was 0.2 mL/min and the gradient was programmed at 95% B (mobile phase A:5 mM ammonium formate in water; mobile phase B: acetonitrile) for 0.5 min, then linearly reduced to 90% in 2 min, then further reduced to 40% in 7 min and maintained for 1 min before increasing to 95% in 2 min with a 1 min re-equilibration period. A Q Exactive Orbitrap mass spectrometer was run in ESI forward mode using Ion Max HESI II, and full mass spectral scans at 100–1500 m/z were obtained with a maximum injection time of 200 ms, five microscopic scans, and an AGC target of 5×10^5 . The decomposition force was set to 70,000. Data analysis was performed by Beijing Qinglian Biotech, Co., Ltd.

Data Processing and Statistical Analysis

All statistical analyses were performed using IBM SPSS Statistics for Windows, version 26.0. Independent samples *t*-tests were used to compare quantitative data that conformed to a normal distribution; Mann–Whitney *U*-tests were used to compare data that did not conform to a normal distribution. Chi-square tests and Fisher's exact tests were used to compare categorical data.

The raw data files were first processed using Progenesis QI software (Waters, Milford, MA, USA), which included sample alignment, peak picking, peak grouping, deconvolution, and final information export. The exported data were further pre-processed using MetaboAnalyst 5.0 (<https://www.metaboanalyst.ca/>) with reference to the publicly available Human Metabolome Database (HMDB) mass spectrometry database (<https://www.hmdb.ca>). Using the multiple reaction monitoring mode of the triple quadrupole mass spectrometer, the signal intensities of the screened characteristic ions were obtained in the detector, and the peak areas of each peak were detected and corrected using MultiQuant software to determine the relative content of the corresponding substances.

Screening for Differential Metabolites

Correlations among the components were calculated using orthogonal projections to latent structure discriminant analysis (OPLS-DA) (SIMCA 14.0, Umetrics, Sweden). Metabolites with differences were initially screened using variable importance in projection (VIP) analysis. The fold-change (FC) values from the univariate analysis were used to further

screen differential metabolites, and non-parametric (Wilcoxon rank-sum) tests were used to assess the significance of the variables.

The selection of discriminant variables was based on three conditions: (1) initial screening of the data in MetaboAnalyst 5.0 software using a *t*-test to select differential metabolites that met the condition of $P < 0.05$; (2) VIP values ≥ 1 ; and (3) $FC > 1.5$ or < 0.5 .

Path Enrichment Analysis

Metabolites differing between the groups were assessed using the Kyoto Encyclopedia of Genes and Genomes (KEGG) (<http://www.genome.jp/kegg>) library and MetaboAnalyst 5.0 (<https://www.metaboanalyst.ca/>) for pathway and Spearman rank correlation analysis.

Results

Comparison of Patient Clinical Features

There were no statistically significant differences in age, gender, duration of diabetes, history of hypertension, history of heart disease or history of hyperlipidemia among the groups ($P > 0.05$). The clinical characteristics of patients in each group are presented in [Table 1](#).

Differential Metabolite Analysis

Differential Metabolites in the PDR and NPDR Groups Compared to the Control Group

Extraction and filtering of mass spectral data to obtain features defined by *m/z*, retention time, and ion intensity included 7360 features in the PDR group compared to the control group and 6298 in the NPDR group compared to the control group. Compared to the control group, the PDR group showed 80 differential metabolites, of which 33 metabolites were upregulated and 47 were downregulated ([Figure 1A](#)), with R^2Y and Q^2 of 0.968 ($P < 0.005$) and 0.709 ($P < 0.005$), respectively, in the OPLS-DA model ([Figure 1B](#)). Compared to the control group, the NPDR group showed 94 differential metabolites, of which 15 were upregulated and 79 were downregulated ([Figure 1C](#)), with R^2Y and Q^2 values of 0.888 ($P=0.04$) and 0.553 ($P<0.005$), respectively, in the OPLS-DA model ([Figure 1D](#)). R^2Y represents the explanatory power, while Q^2 is the result of seven cross-validations and represents the predictive power of the metabolic profiling data. The above model parameters showed that the models of the PDR and control groups and NPDR and control groups had strong reliability.

Differential Metabolites in the PDR Group Compared to the NPDR Group

Extraction and filtering of the mass spectrometry data produced 6633 features, defined by *m/z*, retention time, and ion intensity. Compared with the NPDR group, the PDR group showed 67 differential metabolites, of which 61 were upregulated and six were downregulated ([Figure 2A](#)). In the OPLS-DA model, R^2Y and Q^2 were 0.452 ($P=0.185$) and 0.117 ($P<0.005$), respectively ([Figure 2B](#)), indicating the poor reliability of the developed model in these two groups.

Table 1 Comparisons of the Clinical Characteristics of the Three Groups of Patients

Projects	PDR Group	NPDR Group	Control Group
Age (years)	59.44±0.73	59.81±1.48	62.60±1.42
Gender (M/F)	30/33	19/18	13/17
DM duration (years)	14.00±0.97	12.59±0.99	–
HTN (yes/no)	34/29	18/19	16/14
CAD (yes/no)	14/49	8/29	7/23
DLD (yes/no)	18/45	11/26	9/21

Abbreviations: -, No data available. PDR, proliferative diabetic retinopathy; NPDR, non-proliferative diabetic retinopathy; DM, diabetes mellitus; HTN, hypertension; CAD, coronary artery disease; DLD, Dyslipidemia.

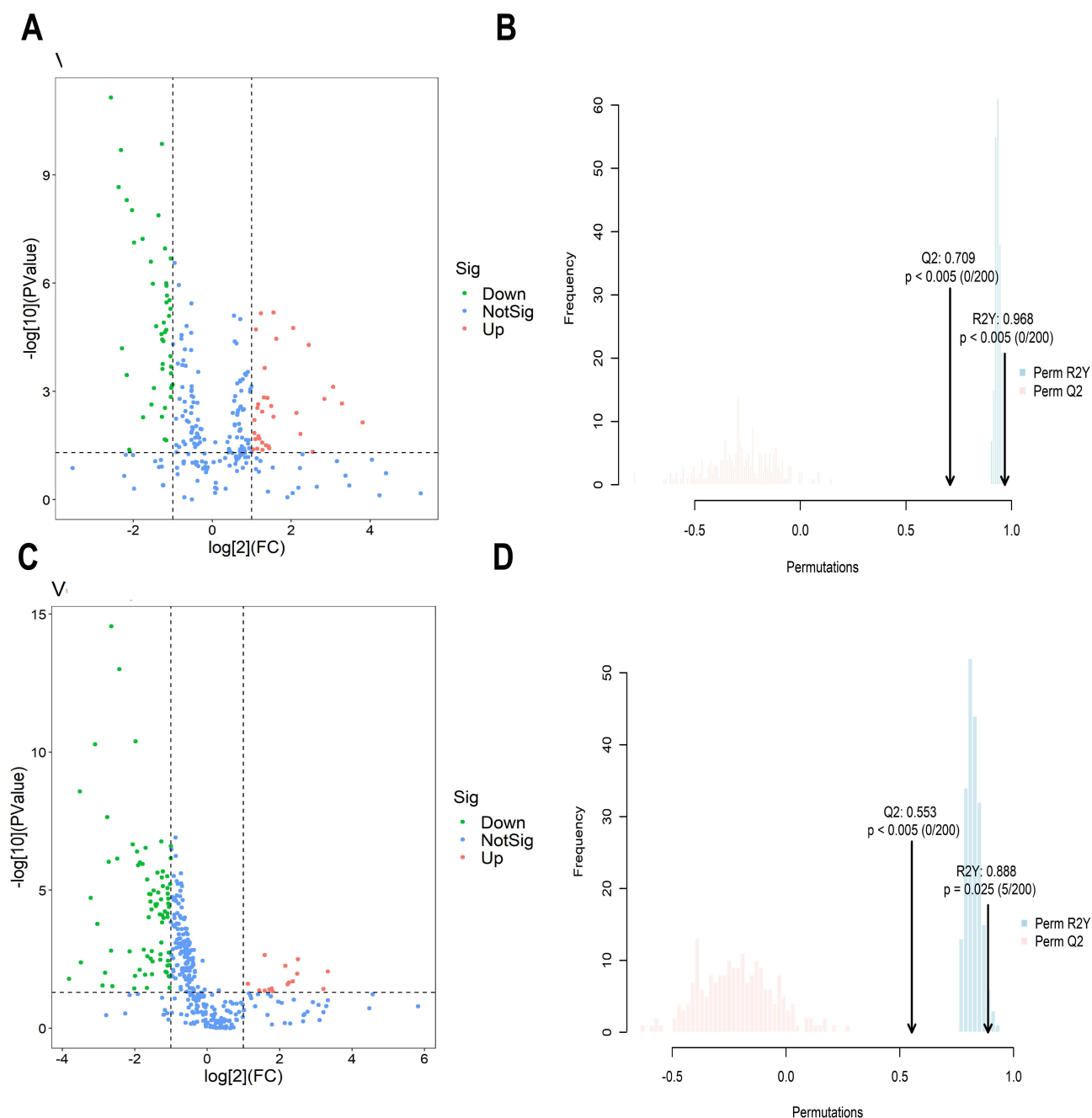


Figure 1 Volcano plot and score plots of the orthogonal projections to latent structure discriminant analysis (OPLS-DA) model. **(A and B)** Metabolic features that differ between the PDR and control groups, showing well separation in the OPLS-DA score plot. **(C and D)** Metabolic features that differ between the NPDR and control groups, showing well separation in the OPLS-DA score plot.

Differential Metabolites in Subgroups Within the PDR Group

Compared to the non-laser group, the laser group showed six differential metabolites, five of which were upregulated: S-(2,4-dinitrophenyl)glutathione, pantothenol, glucoiberin, gamma-glutamylcysteine, CMP-3-deoxy-D-manoctulosonate, and one of which was downregulated: (2R,3S)-2,3-dimethylmalate.

Compared to group a (DM duration <10 years), group b ($10 \leq$ DM duration <20 years) showed five differential metabolites, all of which were upregulated: N-phenylacetylglutamine, L-octanoylcarnitine, dopaxanthin, decanoylcarnitine, and acetyl-N-formyl-5-methoxykynurenamine. Compared to group b, group c (DM duration \geq 20 years) had two

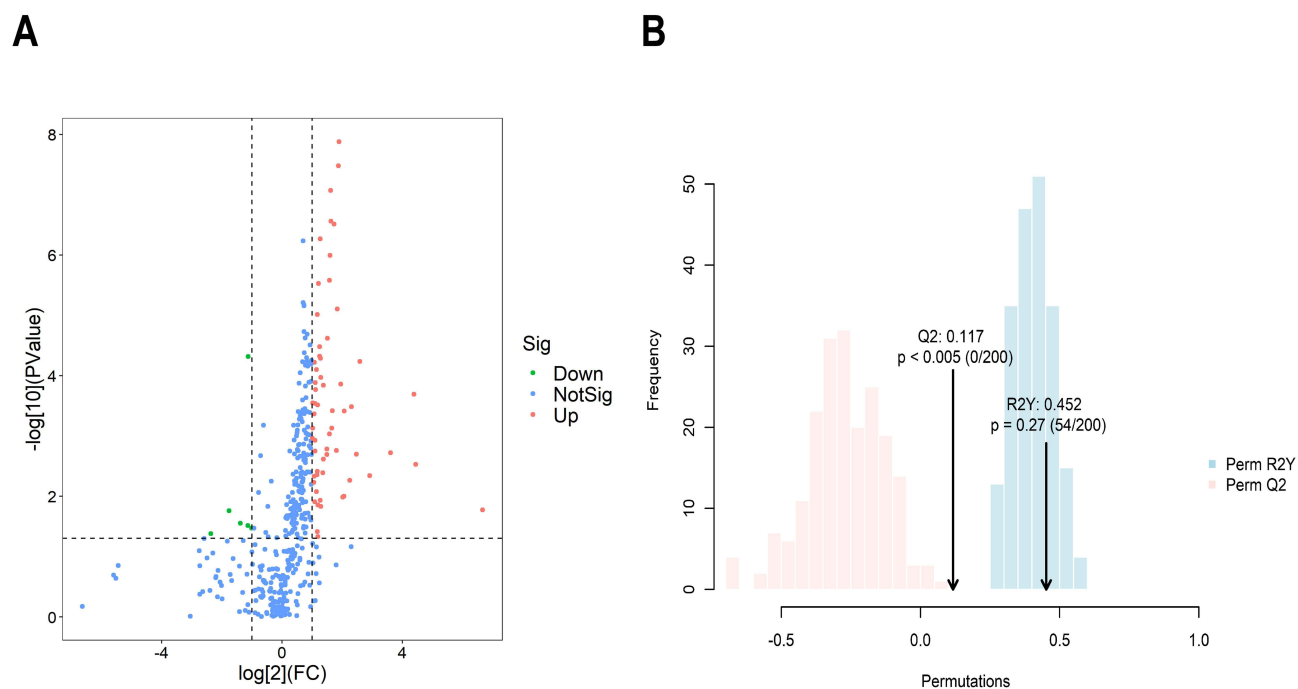


Figure 2 Volcano plot and score plots of the orthogonal projections to latent structure discriminant analysis (OPLS-DA model). (**A** and **B**) Metabolic features that differ between the PDR and NPDR groups, showing little difference in the OPLS-DA score plot.

differential metabolites, both of which were downregulated; (2,4-dinitrophenyl) glutathione and Precorrin-1. Compared to group a, group c had two differential metabolites: D- (+)-maltose (upregulated) and DL-Ethionine (downregulated).

Potential Biomarkers

Receiver operating characteristic (ROC) curves were plotted separately for each potential biomarker by logistic regression analysis. The variables were further confirmed by Mann–Whitney *U*-test, and the differential metabolites with an area under the curve (AUC) of ≥ 0.80 were identified as potential biomarkers ($p < 0.05$) (Table 2).

Table 2 Potential Biomarkers in the PDR and Control Groups, NPDR and Control Groups, and PDR and NPDR Groups

Name	HMDB-ID	VIP	FC	P	Sig
PDR vs Control Groups					
3-methylhistamine	HMDB0001861	3.5909	0.3407	0.0000	Down
N-acetyl-L-histidine	HMDB0032055	2.8948	0.4828	0.0000	Down
Cytosine	HMDB0000630	2.8606	0.4137	0.0000	Down
NPDR vs control groups					
N-acetyl-L-histidine	HMDB0032055	2.1246	0.4996	0.0000	Down
Hypoxanthine	HMDB0000157	2.4035	0.4817	0.0000	Down
PDR vs NPDR groups					
5-hydroxyindole-3-acetic acid	HMDB0000763	3.4999	3.7224	0.0000	Up
l-3-hydroxykynurenine	HMDB0011631	3.2148	3.0726	0.0000	Up

Abbreviations: PDR, proliferative diabetic retinopathy; NPDR, nonproliferative diabetic retinopathy; HMDB, Human Metabolome Database; VIP, variable importance in projection; FC, fold change; Sig, Significance.

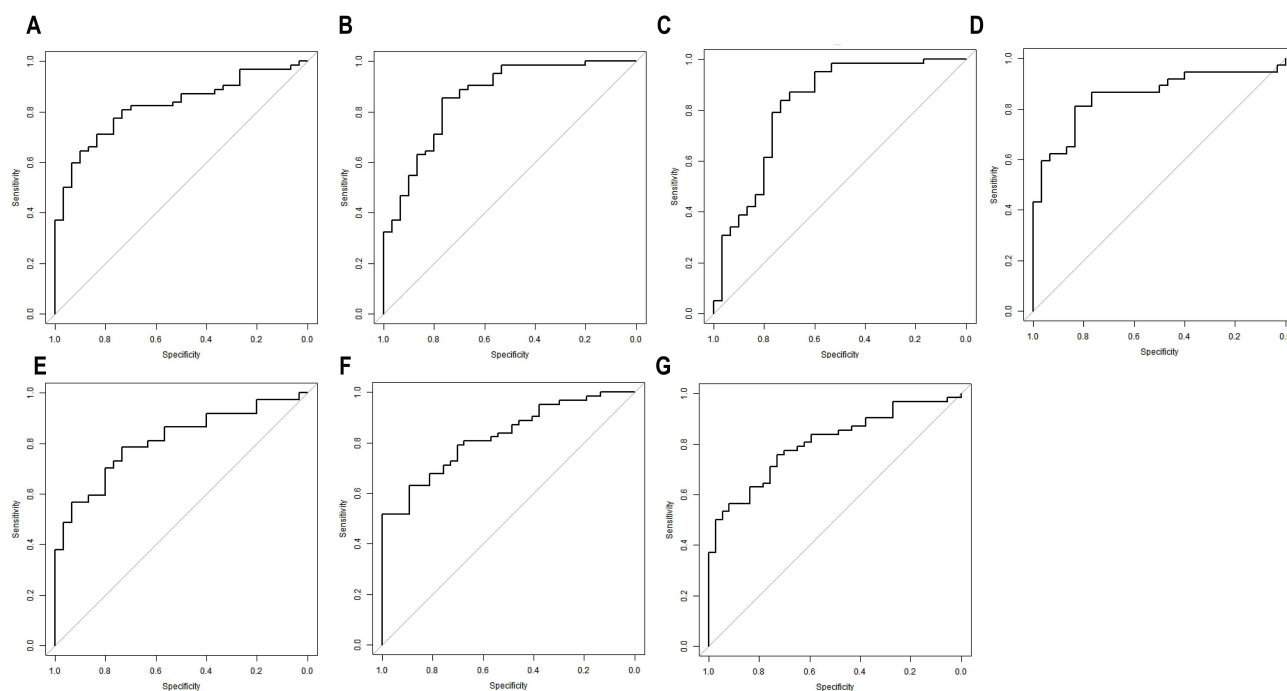


Figure 3 (A–C) ROC curves of n-Acetyl-L-histidine (A), cytosine (B), 3-methylhistamine (C) in groups of the PDR and Control groups. The AUC values for the three markers were 0.82, 0.86 and 0.82, respectively. (D and E) ROC curves of n-acetyl-L-histidine (D) and hypoxanthine (E) in groups of the NPDR and Control groups. The AUC values for the two markers were 0.85 and 0.81, respectively. (F and G) ROC curves of 5-hydroxyindole-3-acetic acid (F) and l-3-hydroxykynurenine (G) in groups of the PDR and NPDR groups. The AUC values for the two markers were 0.82 and 0.80, respectively.

The results showed that for the PDR and Control groups, three potential biomarkers (N-acetyl-L-histidine, cytosine, 3-methylhistamine) were demonstrated, the ROC curve of these three markers was calculated and the corresponding AUC values of 0.82, 0.86, and 0.82, respectively, (Figure 3A–C). For the NPDR and Control groups, two potential biomarkers (N-acetyl-L-histidine, hypoxanthine) were demonstrated, the ROC curve of these two markers was calculated and the corresponding AUC values of 0.85 and 0.81, respectively, (Figure 3D and E). For the PDR and NPDR groups, two potential biomarkers (5-hydroxyindole-3-acetic acid, l-3-hydroxykynurenine) were demonstrated, the ROC curve of these two markers was calculated and the corresponding AUC values of 0.82 and 0.80, respectively, (Figure 3F and G).

Pathway Enrichment Analysis

To identify patterns of biological significance in the metabolomic data, pathway analysis was performed using the MetaboAnalyst software.¹⁶ After detecting metabolites in all samples, further pathway analysis was performed to identify the major biochemical and signal transduction pathways associated with the metabolites. The main metabolic pathways were amino acid metabolism, biosynthesis of other secondary metabolism, chemical structure transformation maps, metabolism of cofactors and vitamins, metabolism of other amino acid, nucleotide metabolism, xenobiotics biodegradation and metabolism, lipid metabolism, energy metabolism, metabolism of terpenoids and polyketides, and carbohydrate metabolism (Figure 4).

The KEGG pathways showed no enrichment of the differential metabolites obtained in both the PDR and NPDR groups compared to the control group. However, the KEGG pathway of the differential metabolites obtained in the PDR group compared to the NPDR group was significantly enriched in the pantothenate and coenzyme A (CoA) biosynthesis pathway ($P=0.0413$), involving the major metabolite pantothenic acid (Figure 5).

Validation of Metabolite Markers

To verify the reliability of the above experimental results, we performed orthogonal targeted metabolomics validation. We collected 90 clinical samples again, including 30 cases in the PDR group, 30 cases in the NPDR group, and 30 cases

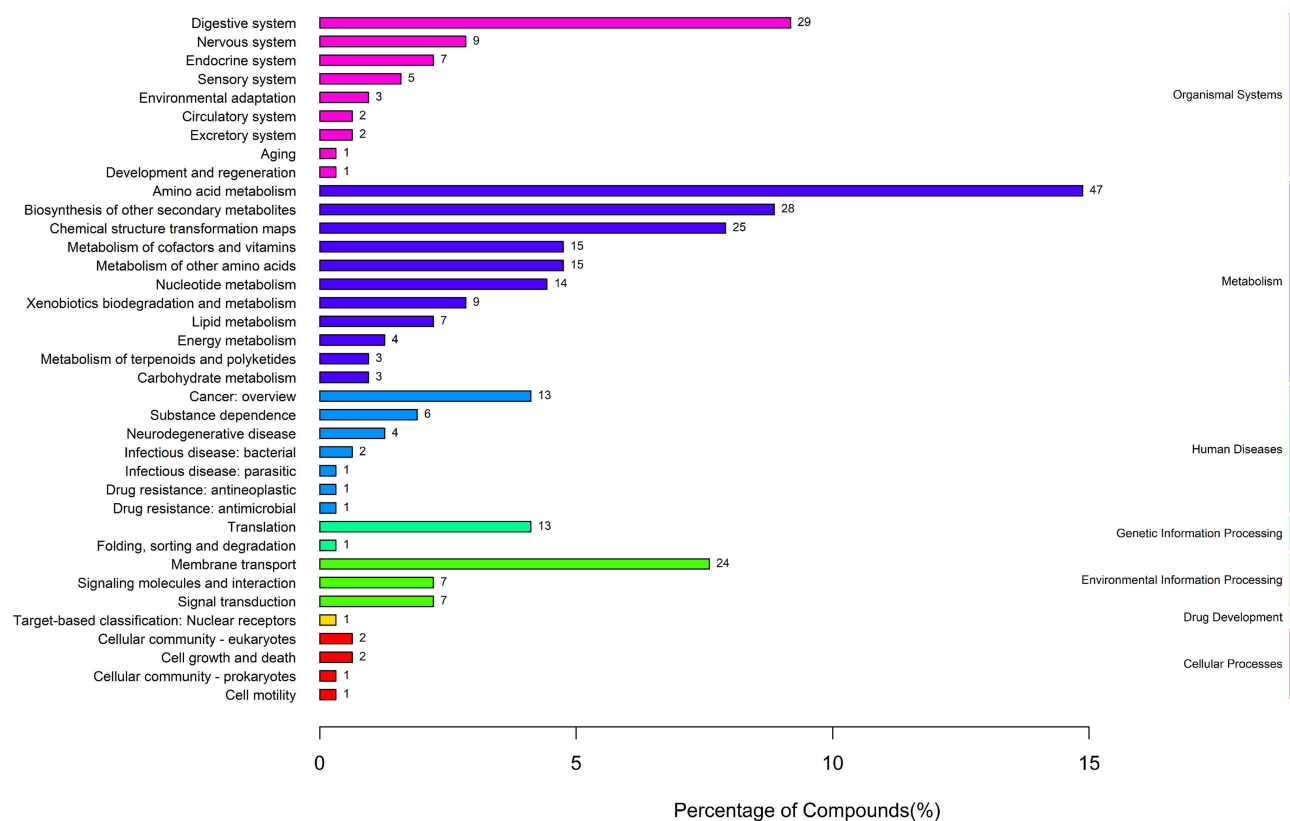


Figure 4 Major biochemical and signal transduction pathways associated with the metabolites. The horizontal coordinates are the number of each metabolite type as a percentage of the total number of entries, while the vertical coordinates are the subclass entries.

in the cataract group. The same instruments described above were used. Targeted qualitative and quantitative detection of amino acid and organic acid metabolites (the selection of categories was based on the proportion of metabolites in each category in the results of the initial experiment, and the two metabolites that accounted for a larger proportion were selected).

Amino acid differential metabolites after two-by-two comparison among the three groups were analyzed by logistic regression, ROC curves were plotted separately, and amino acid differential metabolites satisfying the condition of $AUC \geq 0.75$ were screened by Mann–Whitney *U*-test. The results confirmed that compared with the Control group, the levels of lysine and asparagine in the AH of the PDR group were significantly increased, and the levels of histidine and tyrosine were significantly decreased, and the difference was statistically significant ($P < 0.05$). Compared with the Control group, the level of asparagine was significantly increased and the level of histidine was significantly decreased in the AH of the NPDR group, and the difference was statistically significant ($P < 0.05$). Compared with the NPDR group, no metabolites of amino acids meeting the conditions were found in the AH of the PDR group. In the experimental group, compared with the Control group, the histidine levels in both the PDR and NPDR AH were significantly decreased, and the difference was statistically significant ($P < 0.05$) (Table 3). Thus, the research value of histidine in metabolomics of diabetic retinopathy and the reliability of the data were strongly confirmed.

When targeting and validating the differential metabolites of organic acids, the differential metabolites were also screened with $AUC \geq 0.75$, and the results confirmed that compared with the Control group, the levels of Lactic acid, D-glucuronic acid, and pyroglutamic acid in the AH of the PDR group were significantly increased, and the level of succinic acid decreased significantly, and the difference was statistically significant ($P < 0.05$). Compared with the Control group, the levels of 3-hydroxy-3-methylglutaric acid, D-glucuronic acid, malic acid, and citric acid in the AH of the NPDR group increased significantly, and the difference was statistically significant ($P < 0.05$). Compared with the NPDR group, the levels of 3-hydroxy-3-methylglutaric acid, succinic acid in the AH of the PDR group decreased

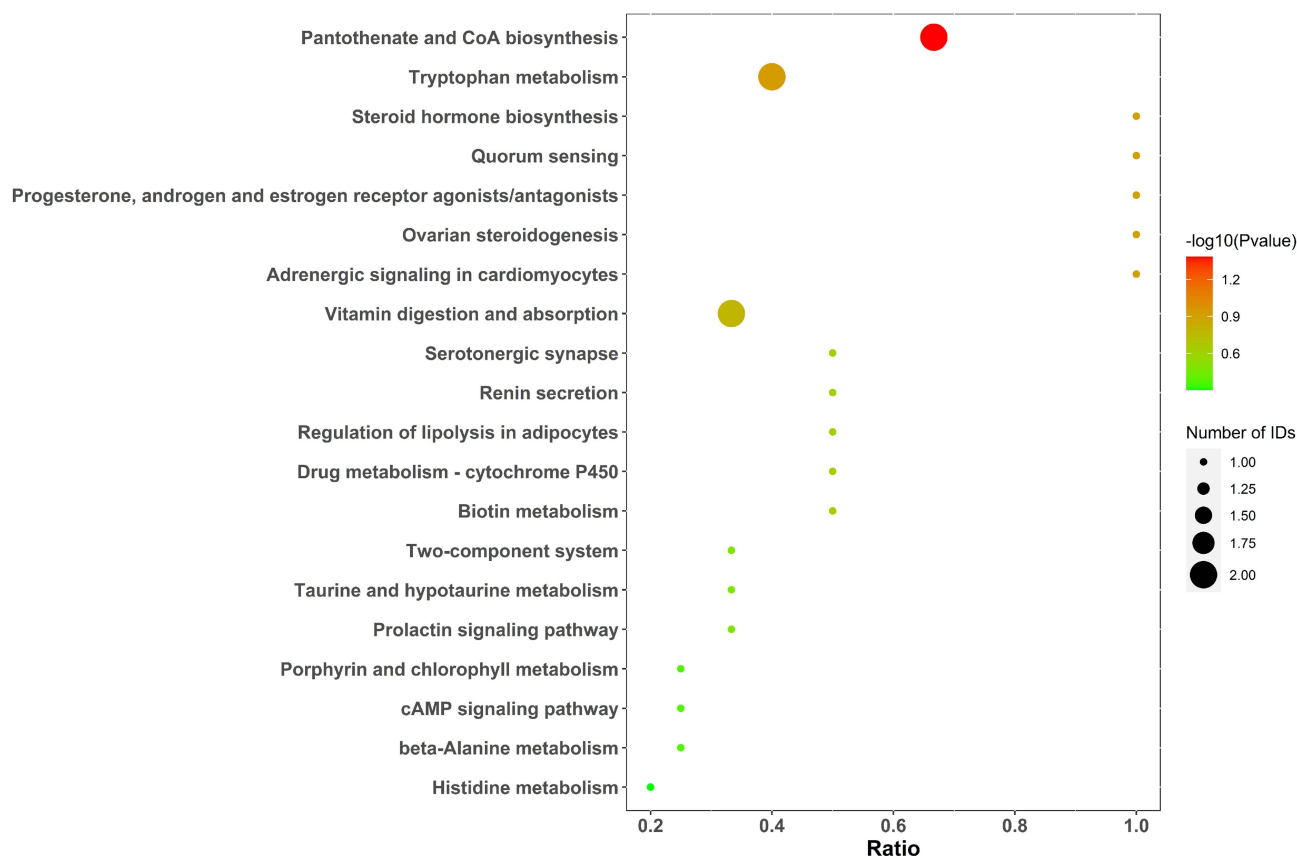


Figure 5 Pathway enrichment analysis. Twenty pathways differed between the nonproliferative diabetic retinopathy (NPDR) and proliferative diabetic retinopathy (PDR) groups; among them, the biosynthetic pathways of pantothenic acid and coenzyme A (CoA) were significantly enriched.

significantly, and the difference was statistically significant ($P < 0.05$). In the experimental group, compared with Control group, the level of organic acid metabolite succinic acid decreased in 80 differential metabolites in PDR group, and the difference was statistically significant ($P < 0.05$). Compared with Control group, the levels of organic acid metabolites malic acid and citric acid in 94 differential metabolites in NPDR group increased significantly, and the difference was statistically significant ($P < 0.05$). Compared with the NPDR group, the levels of organic acid metabolite succinic acid in

Table 3 The Amino Acid-Based Metabolites of the PDR and Control, NPDR and Control in the Validation Experiments

Name	Specificity	Sensitivity	FC	P	AUC	Sig
PDR vs Control Groups						
Histidine	0.7292	0.6670	0.7823	0.0000	0.8280	Down
Lysine	0.7670	0.7330	1.1972	0.0004	0.7980	Up
Tyrosine	0.7020	0.7330	0.8249	0.0014	0.7680	Down
Asparagine	0.7000	0.8000	1.1544	0.0003	0.7520	Up
NPDR vs control groups						
Asparagine	0.8279	0.7000	1.2022	0.0000	0.7980	Up
Histidine	0.6008	0.6670	0.7640	0.0027	0.7290	Down

Abbreviations: PDR, proliferative diabetic retinopathy; NPDR, nonproliferative diabetic retinopathy; FC, fold change; AUC, area under the curve; Sig, Significance.

Table 4 The Organic Acid Metabolites in the PDR and Control, NPDR and Control, and PDR and NPDR Groups in the Validation Experiments

Name	Specificity	Sensitivity	FC	P	AUC	Sig
PDR vs Control Groups						
Lactic acid	0.7500	0.8330	1.0863	0.0284	0.8230	Up
Succinic acid	0.6670	0.9170	0.5641	0.0109	0.8120	Down
D-glucuronic acid	0.7500	0.6670	1.5192	0.0590	0.7970	Up
Pyroglutamic acid	0.6670	0.8330	1.3370	0.0387	0.7670	Up
NPDR vs control groups						
3-hydroxy-3-methylglutaric acid	0.7500	1.0000	2.0958	0.0040	0.8820	Up
D-glucuronic acid	0.6670	0.9170	1.4296	0.0156	0.8230	Up
Malic acid	0.6670	0.8330	1.2661	0.0288	0.7530	Up
Citric acid	0.8330	0.7500	1.1508	0.0697	0.7500	Up
PDR vs NPDR groups						
3-hydroxy-3-methylglutaric acid	0.8330	0.7500	0.6014	0.0483	0.7950	Down
Succinic acid	0.8330	0.7500	0.5936	0.0127	0.7740	Down

Abbreviations: PDR, proliferative diabetic retinopathy; NPDR, nonproliferative diabetic retinopathy; FC, fold change; AUC, area under the curve; Sig, Significance.

67 differential metabolites in the PDR group decreased significantly, and the difference was statistically significant ($P < 0.05$) (Table 4).

Discussion

The long-term hyperglycemic state of patients with DM causes dysfunction in many organs of the body, especially the retina and kidney. The microvascular-rich eye is significantly damaged, which seriously affects patients physical and mental health and quality of life.^{17,18} Numerous treatments are available for diabetic retinopathy: vitrectomy, retinal laser photocoagulation, and vitreous cavity injection of anti-vascular endothelial growth factor drugs.¹⁹ However, when retinopathy progresses to the middle and advanced stages, improvement in visual acuity after treatment is limited and not obvious. Therefore, the in-depth study of potential biomarkers for the occurrence and progression of DR is of great clinical value and social significance to advance DR treatment, and to precisely prevent and treat PDR and NPDR.

We evaluated the effects of these potential biomarkers on DR from several perspectives. We report for the first time that 3-methylhistamine and N-acetyl-L-histidine, which were associated with PDR in metabolomic analysis, may be new biomarkers and potential therapeutic targets. In the healthy state of the retina, nitric oxide (NO) acts as a rapid relaxant of the vascular endothelium, participating in the control of retinal blood flow under basal conditions and mediating the vasodilatory response to different substances such as acetylcholine, bradykinin, histamine, substance P, and insulin.²⁰ However, the high glucose state leads to a disturbance in amino acid metabolism in the retina, leading to reduced NO production, which affects the downstream substance histamine, resulting in endothelial cell dysfunction and impaired vasodilation.⁴ Histamine causes an imbalance in pro- and anti-angiogenic factors in the diabetic retinal pigment epithelium via the H4 receptor/p38 MAPK axis.²¹ Based on our finding of significantly lower 3-methylhistamine and N-acetyl-L-histidine levels in patients in the PDR and NPDR groups than non-DM cataract controls, we speculate that increasing retinal histamine levels may be a potential therapeutic strategy for delaying the progression of DR and PDR.

Similarly, the ROC results suggested that cytosine in AH can be used as a potential biomarker for good differentiation between the PDR and control groups. During DR development, persistent hyperglycemia leads to increased mitochondrial DNA (mtDNA) base mismatches and cytosine hypermethylation and active DNA, which can suppress gene expression.^{22,23} The use of DNA methylation inhibitors (azacytidine or dnmt1-siRNA) prevented hypermethylation of the mismatch repair proteins Mfn2 and Mlh1, thereby improving retinal dysfunction and DR.²³ Compared to non-diabetic cataract controls, the level of unmethylated cytosines in the AH was significantly decreased in patients with PDR;

therefore, we hypothesized that DR could be prevented or reversed by maintaining mitochondrial dynamics and DNA stability, thereby regulating DNA methylation.

Glutathione levels are decreased in diabetic patients compared to patients without DM, especially those with microvascular complications. Imbalance in glutathione metabolism is associated with oxidative stress.²⁴ The concentrations of superoxide dismutase and glutathione peroxidase were significantly reduced in patients with DR after retinal laser photocoagulation.²⁵ We observed significant S-(2,4-dinitrophenyl) glutathione and gamma-glutamylcysteine upregulation in the laser group of patients with PDR. We speculate that this may be the result of retinal oxidative stress caused by the thermal effect of laser photocoagulation.

In terms of whether or not there was a history of retinal laser photocoagulation treatment, the proportion of patients with a long duration of diabetes was greater than that of patients with a short duration. In the present study, we compared longitudinally the duration of diabetes mellitus <10 years, 10 years \leq DM duration <20 years, DM duration \geq 20 years, and the presence or absence of retinal laser photocoagulation, respectively. The results showed that the differential metabolites in group a, group b, and group c grouped according to the duration of diabetes were different in the two-by-two comparisons, and therefore we speculated that the duration of diabetes had an impact on the intraocular metabolic changes.

Since we again collected a limited number of samples and sample content to validate all discrepant metabolites, we chose two categories of metabolites that were more discrepant and accounted for a larger proportion of the samples: amino acids and organic acids. The results showed that compared with Control group, the levels of lysine and asparagine in the AH of PDR group increased significantly, and the levels of histidine and tyrosine decreased significantly, and the difference was statistically significant ($P < 0.05$). Compared with Control group, the level of asparagine in the AH of NPDR group increased significantly and the level of histidine decreased significantly, and the difference was statistically significant ($P < 0.05$). Therefore, it was confirmed that histidine can be used as a potential biomarker for the diagnosis of PDR and NPDR compared to Control group.

This study has several limitations. First, the number of study subjects was small, and no stratified analysis by age or gender was performed. Furthermore, there were differences in the number of patients between groups, which may affect the generalizability of our findings to different patient subgroups. Second, both diabetes and cataract may cause changes in aqueous humor metabolites, compared with healthy participants, diabetic patients are more suitable as the control group. However, due to ethical constraints, we can only select healthy participants with cataracts as the control group. Finally, although we identified potential biomarkers for DR, their predictive performance needs to be further evaluated in a larger, multicenter validation study.

Conclusion

In conclusion, our findings facilitate the further exploration of DR metabolomics and contribute to the development of metabolic biomarkers for prognosis. Further studies with larger sample sizes are required to determine the roles of these potential biomarkers in the onset and progression of DR and PDR. This will enable the development of new therapeutic strategies to prevent or delay DR progression.

Institutional Review Board Statement

This study was approved by the Human Investigation Ethics Committee of the Eye Hospital of Tianjin Medical University and was conducted in accordance with the principles of the Declaration of Helsinki (2022. KY. 39).

Data Sharing Statement

The data that support the findings of this study are available from the corresponding author Bojie Hu, upon reasonable request.

Informed Consent Statement

Informed consent was obtained from all subjects involved in the study.

Author Contributions

All authors made a significant contribution to the work reported, whether that is in the conception, study design, execution, acquisition of data, analysis and interpretation, or in all these areas; took part in drafting, revising or critically reviewing the article; gave final approval of the version to be published; have agreed on the journal to which the article has been submitted; and agree to be accountable for all aspects of the work.

Funding

Supported by a grant from the Natural Science Foundation of Tianjin City (No. S20ZXD011), Beijing natural science foundation-Beijing Tianjin Hebei basic research cooperation project (J200006), Tianjin Key Medical Discipline (Specialty) Construction Project (TJYXZDXK-037A) and The Science&Technology Development Fund of Tianjin Education Commission for Higher Education (No. 2022ZD058).

Disclosure

The authors have declared that there are no conflicts of interest in this work.

References

- Xuan Q, Ouyang Y, Wang Y, et al. Multiplatform metabolomics reveals novel serum metabolite biomarkers in diabetic retinopathy subjects. *Adv Sci*. 2020;7(22):2001714. doi:10.1002/advs.202001714
- Trott M, Driscoll R, Pardhan S. Associations between diabetic retinopathy, mortality, disease, and mental health: an umbrella review of observational meta-analyses. *BMC Endocr Disord*. 2022;22(1):311. doi:10.1186/s12902-022-01236-8
- Yun JH, Kim JM, Jeon HJ, et al. Metabolomics profiles associated with diabetic retinopathy in type 2 diabetes patients. *PLoS One*. 2020;15(10):e0241365. doi:10.1371/journal.pone.0241365
- Wang H, Fang J, Chen F, et al. Metabolomic profile of diabetic retinopathy: a GC-TOFMS-based approach using vitreous and aqueous humor. *Acta Diabetol*. 2020;57(1):41–51. doi:10.1007/s00592-019-01363-0
- Pietrowska K, Dmuchowska DA, Samczuk P, et al. LC-MS-based metabolic fingerprinting of aqueous humor. *J Anal Methods Chem*. 2017;2017:6745932. doi:10.1155/2017/6745932
- Chen X, Chen Y, Wang L, et al. Metabolomics of the aqueous humor in patients with primary congenital glaucoma. *Mol Vis*. 2019;25:489–501.
- Liew G, Lei Z, Tan G, et al. Metabolomics of Diabetic Retinopathy. *Curr Diab Rep*. 2017;17(11):102. doi:10.1007/s11892-017-0939-3
- Pietrowska K, Dmuchowska DA, Krasnicki P, et al. An exploratory LC-MS-based metabolomics study reveals differences in aqueous humor composition between diabetic and non-diabetic patients with cataract. *Electrophoresis*. 2018;39(9–10):1233–1240. doi:10.1002/elps.201700411
- Misra BB. New software tools, databases, and resources in metabolomics: updates from 2020. *Metabolomics*. 2021;17(5):49. doi:10.1007/s11306-021-01796-1
- Dehdashtian E, Mehrzadi S, Yousefi B, et al. Diabetic retinopathy pathogenesis and the ameliorating effects of melatonin; involvement of autophagy, inflammation and oxidative stress. *Life Sci*. 2018;193:20–33. doi:10.1016/j.lfs.2017.12.001
- Jin H, Zhu B, Liu X, et al. Metabolic characterization of diabetic retinopathy: an (1)H-NMR-based metabolomic approach using human aqueous humor. *J Pharm Biomed Anal*. 2019;174:414–421. doi:10.1016/j.jpba.2019.06.013
- Haines NR, Manoharan N, Olson JL, et al. Metabolomics analysis of human vitreous in diabetic retinopathy and rhegmatogenous retinal detachment. *J Proteome Res*. 2018;17(7):2421–2427. doi:10.1021/acs.jproteome.8b00169
- Sinclair AJ, Girling AJ, Gray L, et al. Disturbed handling of ascorbic acid in diabetic patients with and without microangiopathy during high dose ascorbate supplementation. *Diabetologia*. 1991;34(3):171–175. doi:10.1007/BF00418271
- Islam MT. Angiostatic effects of ascorbic acid: current status and future perspectives. *Angiogenesis*. 2020;23(3):275–277. doi:10.1007/s10456-020-09719-9
- Sumarriva K, Uppal K, Ma C, et al. Arginine and carnitine metabolites are altered in diabetic retinopathy. *Invest Ophthalmol Vis Sci*. 2019;60(8):3119–3126. doi:10.1167/iovs.19-27321
- Wang X, Zhang A, Yan G, et al. Metabolomics and proteomics annotate therapeutic properties of geniposide: targeting and regulating multiple perturbed pathways. *PLoS One*. 2013;8(8):e71403. doi:10.1371/journal.pone.0071403
- Tan GS, Ikram MK, Wong TY. Traditional and novel risk factors of diabetic retinopathy and research challenges. *Curr Med Chem*. 2013;20(26):3189–3199. doi:10.2174/09298673113209990023
- Hong SJ, Kim ST, Kim TJ, et al. Cellular and molecular changes associated with inhibitory effect of pioglitazone on neointimal growth in patients with type 2 diabetes after zotarolimus-eluting stent implantation. *Arterioscler Thromb Vasc Biol*. 2010;30(12):2655–2665. doi:10.1161/ATVBAHA.110.212670
- Wang W, Lo A. Diabetic retinopathy: pathophysiology and treatments. *Int J Mol Sci*. 2018;19(6). doi:10.3390/ijms19061816
- Schmetterer L, Polak K. Role of nitric oxide in the control of ocular blood flow. *Prog Retin Eye Res*. 2001;20(6):823–847. doi:10.1016/s1350-9462(01)00014-3
- Lee BJ, Byeon HE, Cho CS, et al. Histamine causes an imbalance between pro-angiogenic and anti-angiogenic factors in the retinal pigment epithelium of diabetic retina via H4 receptor/p38 MAPK axis. *BMJ Open Diabetes Res Care*. 2020;8(2):e001710. doi:10.1136/bmjdr-2020-001710
- Mishra M, Kowluru RA. DNA methylation—a potential source of mitochondria DNA base mismatch in the development of diabetic retinopathy. *Mol Neurobiol*. 2019;56(1):88–101. doi:10.1007/s12035-018-1086-9
- Kowluru RA, Mohammad G. Epigenetics and mitochondrial stability in the metabolic memory phenomenon associated with continued progression of diabetic retinopathy. *Sci Rep*. 2020;10(1):6655. doi:10.1038/s41598-020-63527-1

24. Lutchmansingh FK, Hsu JW, Bennett FI, et al. Glutathione metabolism in type 2 diabetes and its relationship with microvascular complications and glycemia. *PLoS One*. 2018;13(6):e0198626. doi:10.1371/journal.pone.0198626
25. Galetović D, Bojić L, Bućan K, et al. The role of oxidative stress after retinal laser photocoagulation in nonproliferative diabetic retinopathy. *Coll Antropol*. 2011;35(3):835–840.

Diabetes, Metabolic Syndrome and Obesity

Dovepress
Taylor & Francis Group

Publish your work in this journal

Diabetes, Metabolic Syndrome and Obesity is an international, peer-reviewed open-access journal committed to the rapid publication of the latest laboratory and clinical findings in the fields of diabetes, metabolic syndrome and obesity research. Original research, review, case reports, hypothesis formation, expert opinion and commentaries are all considered for publication. The manuscript management system is completely online and includes a very quick and fair peer-review system, which is all easy to use. Visit <http://www.dovepress.com/testimonials.php> to read real quotes from published authors.

Submit your manuscript here: <https://www.dovepress.com/diabetes-metabolic-syndrome-and-obesity-journal>